IMMUNOLOGY

Food antigens drive spontaneous IgE elevation in the absence of commensal microbiota

Sung-Wook Hong[1]*†, Eunju O[1,2], Jun Young Lee[1,2], Minji Lee[1,2], Daehee Han[1], Hyun-Ja Ko[1], Jonathan Sprent[3,4], Charles D. Surh[1,2]‡, Kwang Soon Kim[1,2]†

Immunoglobulin E (IgE), a key mediator in allergic diseases, is spontaneously elevated in mice with disrupted commensal microbiota such as germ-free (GF) and antibiotics-treated mice. However, the underlying mechanisms for aberrant IgE elevation are still unclear. Here, we demonstrate that food antigens drive spontaneous IgE elevation in GF and antibiotics-treated mice by generating T helper 2 (T_H2)–skewed T follicular helper (T_{FH}) cells in gut-associated lymphoid tissues (GALTs). In these mice, depriving contact with food antigens results in defective IgE elevation as well as impaired generation of T_{FH} cells and IgE-producing cells in GALT. Food antigen–driven T_{FH} cells in GF mice are mostly generated in early life, especially during the weaning period. We also reveal that food antigen–driven T_{FH} cells in GF mice are actively depleted by colonization with commensal microbiota. Thus, our findings provide a possible explanation for why the perturbation of commensal microbiota in early life increases the occurrence of allergic diseases.

INTRODUCTION

Immunoglobulin E (IgE) is a key mediator for allergic reactions to innocuous foreign antigens (Ags), despite its beneficial role in protection against parasite infection (1). In healthy individuals, serum IgE is rare relative to other isotypes and is tightly regulated to avoid excessive allergic responses. IgE elevation is generally observed in allergic patients, contributing to the pathophysiology of allergic disease. Degranulation of mast cells and basophils by allergen-mediated IgE/FceR cross-linking causes fatal allergic symptoms (1). Furthermore, circulating IgE promotes hematopoiesis of basophils and survival of mast cells, the effector cells mediating allergic symptoms (2, 3).

Commensal microbiota profoundly influence host physiology. Perturbation of commensal microbiota is widely believed to be one of the major causative factors in allergic diseases (4). Experimental evidence has shown that the commensal microbiota plays a critical role in suppressing aberrant IgE production. Serum IgE levels are abnormally elevated in germ-free (GF) mice or conventional mice treated with broad-spectrum antibiotics (ABX) (2, 5). However, the underlying mechanisms for spontaneous IgE elevation in GF mice, including the responsible Ags and immune subsets involved, remain to be elucidated.

T follicular helper (T_{FH}) cells are a specialized $CD4^+$ T cell subset for helping B cell immunity (6). After engaging with Ag-bearing dendritic cells (DCs), $CD4^+$ T cells commit to differentiation into T_{FH} cells by expressing BCL-6, a key transcription factor orchestrating T_{FH} cell differentiation (7, 8). T_{FH}-committed T cells migrate into the T-B border and B cell follicles, and fully differentiate into $PD-1^{hi}$ $CXCR5^+$ germinal center (GC) T_{FH} cells (9). In mice infected with helminths and sensitized with allergens, interleukin-4 (IL-4)–producing T_{FH} cells were effectively generated; these T_{FH} cells, rather than conventional T helper (T_H2) cells, are mainly required for IgE production (10, 11). In contrast, IgE can be elevated in a T_{FH} cell–independent manner, as shown in BCL-6–deficient mice (12). Although IgE elevation in GF mice is dependent on $CD4^+$ T cells and IL-4 (5), it is unclear whether spontaneous IgE elevation observed in GF mice is mediated by T_{FH} cells or caused by T_{FH} cell–independent mechanisms.

In this study, we demonstrate that IgE elevation in GF and ABX-treated mice is not a direct result of the absence of intestinal microbiota but is induced by aberrant immune responses to ingested food Ags. We show that GF mice deprived of contact with food Ags have basal IgE levels. In GF mice, food Ag–specific T_{FH} cells are found predominantly in mesenteric lymph nodes (MLNs) and Peyer's patches (PPs) and are major producers of IL-4. T_{FH} cells are required for food Ag–driven IgE elevation in the absence of commensal microbiota. Food Ag–driven T_{FH} cells in GF mice are mostly generated in early life, especially during the weaning period, and actively depleted by colonization with commensal microbiota. Furthermore, we reveal that, although food Ag–driven T_{FH} cell development is crucial for initial IgE production, prolonged maintenance of IgE is largely due to generation of long-lived IgE-producing plasma cells.

RESULTS

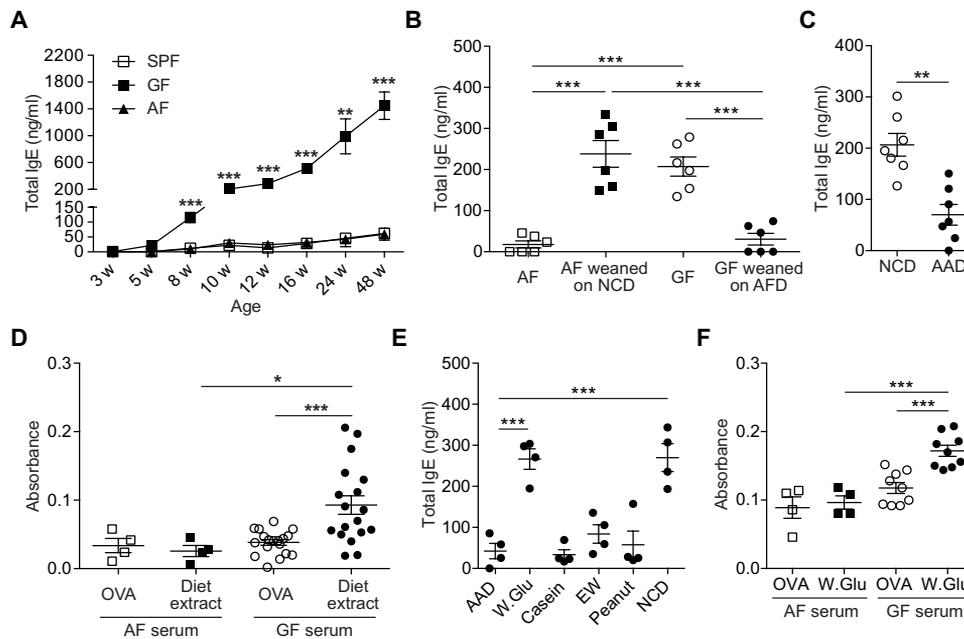### Ingested food Ags are responsible for spontaneous IgE elevation in GF mice

To investigate the role of ingested food Ags in spontaneous IgE elevation in GF mice, we examined serum IgE levels in "Ag-free (AF)" mice, i.e., F1 offspring of GF breeders raised on a diet devoid of macromolecules such as proteins and polysaccharides [AF diet (AFD)] (13). These F1 mice were raised on AFD. As reported previously (5), notable elevation of serum IgE levels in GF mice with age was detected after weaning mice onto normal chow diet (NCD), whereas serum IgE levels remained at basal level (<100 ng/ml) in specific pathogen–free (SPF) mice (Fig. 1A). In contrast to GF mice, AF mice had basal serum IgE levels (<100 ng/ml) comparable to those in SPF mice (Fig. 1A). IgE elevation was not observed in GF mice

Fig. 1. Ingested food Ags are responsible for spontaneous IgE elevation in GF mice. (**A**) Serum IgE levels of SPF, GF, and AF mice with ages were measured by enzyme-linked immunosorbent assay (ELISA) ($n = 4$). Statistically significant difference between GF and AF mice at indicated age was shown. (**B**) AF and GF pups were weaned onto NCD (AF weaned on NCD) and AF diet (GF weaned on AFD), respectively. After 7 weeks of feeding, serum IgE levels were measured by ELISA. Age-matched AF and GF mice were used as control mice ($n = 6$). (**C**) GF mice were weaned onto NCD or AAD. After 6 weeks, serum IgE levels were measured by ELISA ($n = 7$). (**D**) Levels of IgE specific to water-soluble fraction of chow diet (diet extract) in sera from 12-week-old AF and GF mice were measured by direct ELISA. OVA at an equivalent amount was used as an irrelevant control ($n = 4$ for AF sera and $n = 18$ for GF sera). (**E**) GF mice were weaned onto AAD mixed with indicated proteins (W.Glu: wheat gluten and EW). After 6 weeks of feeding, serum IgE levels were measured by ELISA ($n = 4$). Each symbol represents an individual mouse. (**F**) Levels of serum IgE specifically bound to wheat gluten ($n = 4$ for AF sera and $n = 9$ for GF sera). Data in (A) and (E) are representative data of two or three independent experiments. Data are pooled from two or three independent experiments (B, C, D, and F). Statistical differences were determined by one-way analysis of variance (ANOVA) with Tukey's multiple comparisons test (A, B, and D to F) or by unpaired two-tailed Student's *t* test (C). *$P < 0.05$, **$P < 0.01$, ***$P < 0.001$. Error bars represent SEM.

weaned onto AFD; conversely, in AF mice weaned onto sterile NCD, serum IgE levels were as high as in age-matched normal GF mice (Fig. 1B).

To exclude the possibility that the absence of IgE elevation in AF mice and GF mice weaned onto AFD was caused by an artifact of the AFD, GF mice were weaned onto a commercially available sterile amino acid diet (AAD). AAD is devoid of protein Ags as the result of replacing protein components with a mixture of amino acids. GF mice fed with AAD for 6 weeks after weaning failed to display the elevation of serum IgE (Fig. 1C), confirming that aberrant IgE elevation in GF conditions is caused by ingested food Ags.

In accordance with these findings, in GF mice, serum IgE specifically bound to diet extracts was significantly higher relative to IgE bound to an irrelevant Ag, ovalbumin (OVA), and that of AF mice (Fig. 1D). Furthermore, in GF mice raised on AAD alone or mixed with individual food proteins such as wheat gluten, casein, egg white (EW), and peanut, IgE elevation was observed only in wheat gluten–fed mice (Fig. 1E). Wheat gluten is a component of NCD. Hence, serum IgE specifically bound to wheat gluten in GF mice was higher than IgE bound to OVA (Fig. 1F). These results suggest that not all food Ags are capable of inducing IgE elevation and that distinct immunogenic properties of food Ags determine IgE elevation in GF mice. Collectively, our data indicate that spontaneous IgE elevation in GF mice is driven by specific immune responses to individual food Ags, rather than a nonspecific consequence of GF conditions as proposed previously (*5*, *14*).

Food Ags induce T$_H$2-skewed immune responses in MLN and PP in GF conditions

In accordance with a previous study (*5*), CD4$^+$ T cells were found to be crucial for IgE elevation in GF mice, as serum IgE levels were decreased by depleting CD4$^+$ T cells (fig. S1A). We found that relative to SPF and GF mice, CD44^{hi} activated CD4$^+$ T cells in AF mice were profoundly reduced in gut-associated lymphoid tissues (GALTs) such as MLN and PP (fig. S1, B and C). In GF mice, relative to SPF mice, CD4$^+$ T cells in MLN and PP were more polarized into IL-4–producing cells, which are essential for IgE production (*15*), but IL-4–producing CD4$^+$ T cells were significantly reduced in AF mice (fig. S1D). Reduction of IL-4–producing CD4$^+$ T cells was not caused by the reciprocal increase of Foxp3$^+$ regulatory CD4$^+$ T (T$_{reg}$) cells because the number of T$_{reg}$ cells was also significantly reduced in AF mice relative to GF and SPF mice (fig. S1E). These results suggest that food Ags are responsible for the generation of IL-4–producing CD4$^+$ T cells in MLN and PP in GF mice.

Food Ag–driven IL-4–producing T$_{FH}$ cells in MLN and PP are key mediators of IgE elevation in GF mice

The T$_{FH}$ cell subset is a key mediator for antibody production and is also involved in IgE production (*10*, *11*). To elucidate the role of T$_{FH}$ cells in spontaneous food Ag–driven IgE production in GF mice, we examined T$_{FH}$ cell populations in MLN and PP, where CD4$^+$ T cells are activated in response to food Ags. In GF mice, PD-1^{hi} CXCR5$^+$ T$_{FH}$ cell populations were abundant among CD44^{hi} activated CD4$^+$ T cells in MLN and PP relative to SPF mice (Fig. 2A). Despite the higher frequency of
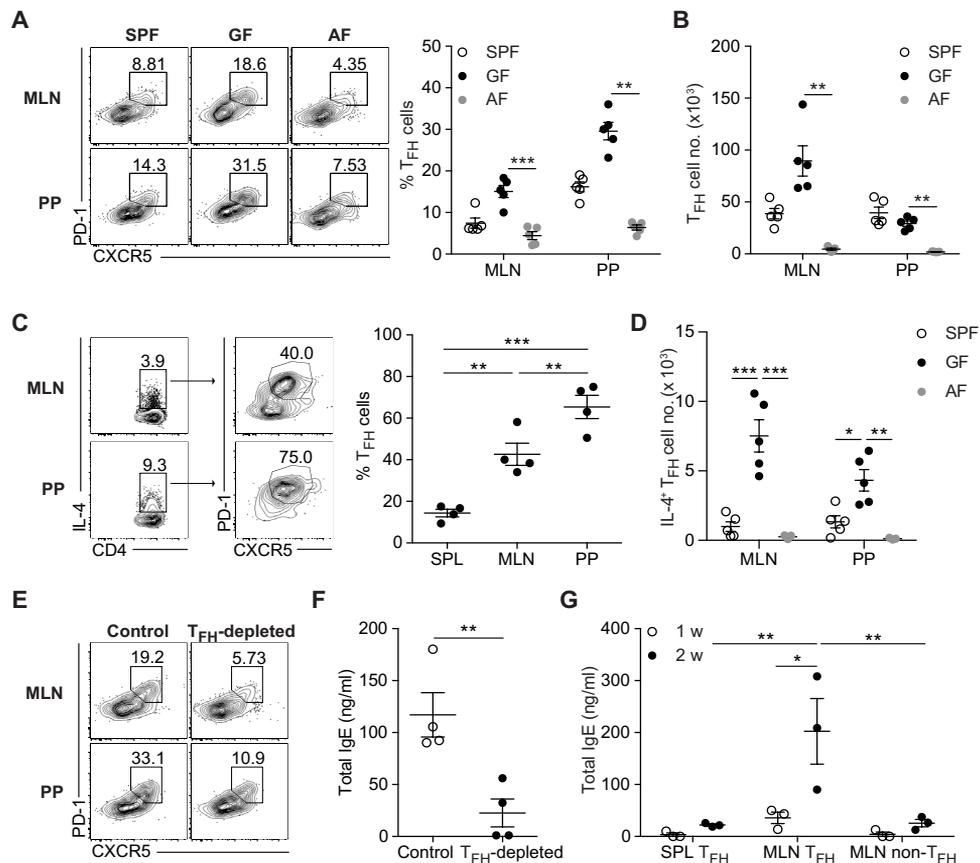
Fig. 2. Food Ag–driven T$_{FH}$ cells generated in GALT mediate IgE elevation in GF conditions. (**A** to **C**) Single-cell suspension was prepared from MLN and PP from 10-week-old SPF, GF, and AF mice. (A) Representative fluorescence-activated cell sorting (FACS) plot of CXCR5 and PD-1 (left) and frequency of PD-1^{hi} CXCR5$^+$ T$_{FH}$ cells (right) gated on CD4$^+$ TCRβ$^+$ Foxp3$^-$ CD44^{hi} cells ($n = 5$). (B) Number of PD-1^{hi} CXCR5$^+$ T$_{FH}$ cells at indicated tissues. (C) Representative FACS plot showing PD-1^{hi} CXCR5$^+$ T$_{FH}$ cells among IL-4$^+$ CD4$^+$ T cells (left) and frequency of PD-1^{hi} CXCR5$^+$ T$_{FH}$ cells gated on IL-4–producing CD4$^+$ T cells in indicated tissues from 10-week-old GF mice ($n = 4$) (right). (**D**) Number of IL-4–producing T$_{FH}$ cells in indicated tissues from SPF, GF, and AF mice. (**E** and **F**) GF mice (4.5 weeks old) were treated with isotype (Control) or anti-ICOSL antibody (T$_{FH}$-depleted) every 3 days for 3 weeks to deplete T$_{FH}$ cells. Representative FACS plot showing PD-1^{hi} CXCR5$^+$ T$_{FH}$ cells in MLN and PP (E) and serum IgE levels ($n = 4$) (F). (**G**) FACS-sorted T$_{FH}$ cells and non-T$_{FH}$ cells in MLN and T$_{FH}$ cells in SPL from 9- to 12-week-old GF mice were cotransferred into GF $Rag1^{-/-}$ mice with naïve B cells isolated from SPF mice. Serum IgE levels at 1 and 2 weeks after transfer were shown ($n = 3$). Each symbol represents an individual mouse. Data are pooled from two independent experiments (A and B). Data in (C), (D), (F), and (G) are representative of two or three independent experiments. Statistical differences were determined by one-way (A to D) or two-way (G) ANOVA with Tukey's multiple comparisons test or by unpaired two-tailed Student's t test (F). *$P < 0.05$, **$P < 0.01$, ***$P < 0.001$. Error bars represent SEM.

T$_{FH}$ cells in both MLN and PP of GF mice, the number of T$_{FH}$ cells in PP in GF mice was comparable with that in SPF mice, presumably due to reduced size and cellularity of PP in GF mice (Fig. 2B). The emergence of T$_{FH}$ cells in GALT of GF mice was observed upon weaning of mice onto NCD (fig. S2A). In contrast to the high levels of T$_{FH}$ cells in GF mice, both the percentage and number of T$_{FH}$ cells were profoundly reduced in MLN and PP of AF mice, indicating that food Ags are responsible for the generation of T$_{FH}$ cells in GALT in GF conditions (Fig. 2, A and B). Consistent with the defective T$_{FH}$ cell generation in AF mice, GC B cell generation, which is mainly mediated by T$_{FH}$ cells, was profoundly reduced in MLN and PP of AF mice (fig. S2B).

In T$_H$2-skewed conditions, T$_{FH}$ cells are known to produce a T$_H$2 signature cytokine, IL-4 (*16*, *17*). In accordance with these studies, about 40 and 70% of IL-4–producing CD4$^+$ T cells in MLN and PP, respectively, were PD-1^{hi} CXCR5$^+$ T$_{FH}$ cells, whereas only 20% were T$_{FH}$ cells in spleen (SPL) (Fig. 2C). IL-4–producing T$_{FH}$ cells were profoundly increased in GF mice relative to SPF mice but markedly reduced in AF mice, suggesting that IL-4–producing T$_{FH}$ cells are generated in

response to food Ags in GF conditions (Fig. 2D). Furthermore, IgE-producing plasma cells were detected only in MLN and PP of GF mice by means of enzyme-linked immunospot (ELISPOT) assay, but not in AF mice (fig. S2, C and D). To further elucidate the critical role of T$_{FH}$ cells in IgE elevation in GF mice, young GF mice were treated with anti-ICOSL antibody to prevent the generation of T$_{FH}$ cells (*8*, *18*). By blocking ICOS-ICOSL (inducible T cell co-stimulator – ICOS ligand) interaction, food Ag–induced T$_{FH}$ cell generation was greatly reduced and IgE elevation was consequently suppressed (Fig. 2, E and F). Furthermore, transfer of T$_{FH}$ cells from MLN of GF mice, but not of non-T$_{FH}$ cells from MLN or splenic T$_{FH}$ cells, led to the efficient increase of serum IgE levels in GF $Rag1^{-/-}$ mice cotransferred with naïve B cells (Fig. 2G). IgE specifically bound to wheat gluten was also increased in GF $Rag1^{-/-}$ mice reconstituted with naïve B cells by the transfer of MLN T$_{FH}$ cells but not by the transfer of SPL T$_{FH}$ cells or MLN non-T$_{FH}$ cells (fig. S3). Collectively, these results indicate that IL-4–producing T$_{FH}$ cells generated in response to food Ags, especially in MLN, are critical for IgE elevation in GF mice.

DCs initiate food Ag–driven T_{FH} cell differentiation in GF mice by elevating ICOS expression on activated T cells via CD40-CD40L interaction

Next, to define the underlying mechanisms for the generation of food Ag–driven T_{FH} cells in GF mice, we first examined ICOS expression on CD4^{+} T cells because ICOS expressed on CD4^{+} T cells is critical for T_{FH} cell differentiation (18, 19). In GF mice, ICOS expression levels on CD44^{hi} activated CD4^{+} T cells were considerably higher in MLN and PP relative to those in SPL (Fig. 3A). Moreover, in AF mice, ICOS expression on activated CD4^{+} T cells in MLN and PP was significantly lower relative to GF mice regardless of the presence of T_{FH} cells (Fig. 3A and fig. S4A). These results show that ICOS is up-regulated in CD4^{+} T cells activated by food Ags in MLN and PP of GF mice.

ICOS expression on CD4^{+} T cells is known to be up-regulated through stimulation by DCs (7). Examination of costimulatory molecules on DCs in GALT of GF and AF mice revealed that the expression of CD40, but not other costimulatory molecules, was significantly reduced in DCs from MLN and PP of AF mice relative to those in GF mice (Fig. 3B and fig. S5). In contrast, the expression levels of CD40 on B cells in MLN and PP were comparable between GF and AF mice (Fig. 3B). Blocking CD40-CD40L interaction substantially reduced ICOS expression on activated CD4^{+} T cells in MLN and PP of GF mice (Fig. 3C) and consequently suppressed food Ag–driven T_{FH} cell generation (Fig. 3, D and E). As a result of defective generation of T_{FH} cells, IgE levels in GF mice treated with anti-CD40L antibody were profoundly reduced relative to GF mice treated with isotype antibody (Fig. 3F). These results suggest that CD40 up-regulated on DCs by exposure to NCD is a key molecule for ICOS up-regulation on CD4^{+} T cells activated by food Ags.
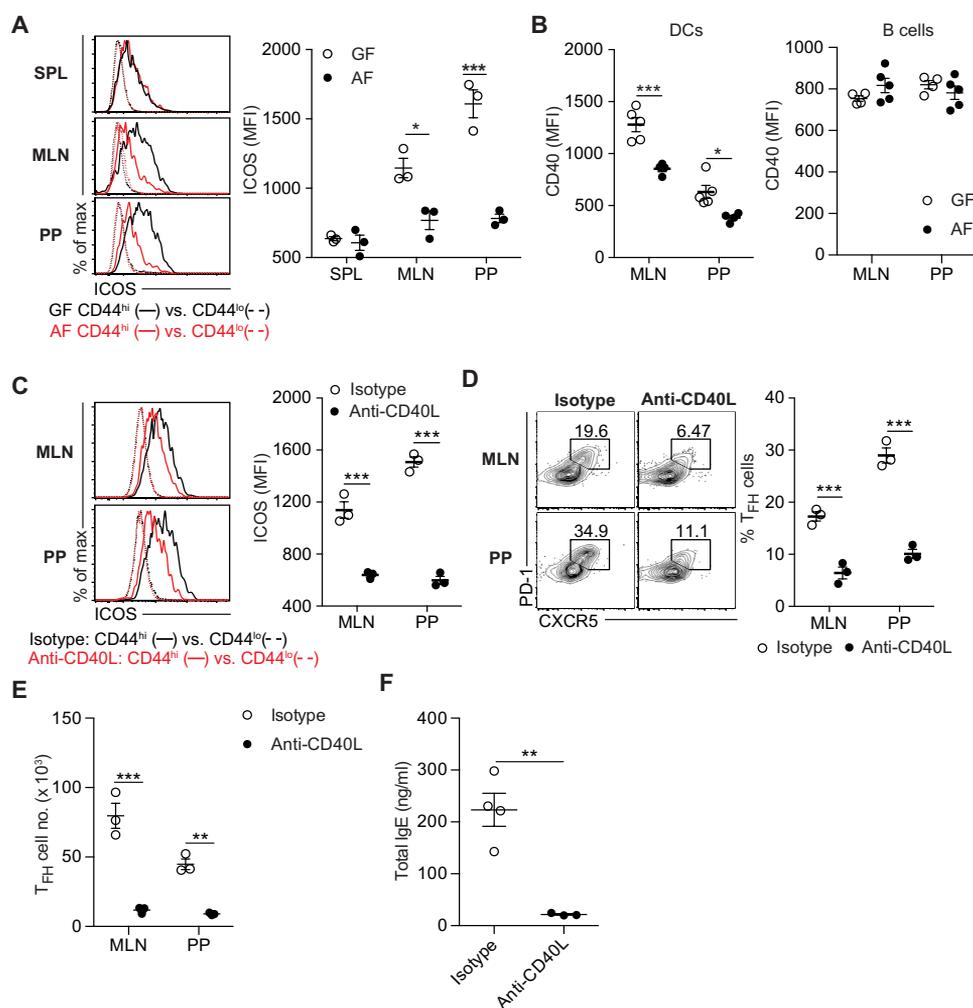
Fig. 3. Food Ag–induced CD40 elevation on DCs promotes ICOS up-regulation on activated T cells. (**A**) Representative histograms (left) and mean fluorescence intensity (MFI) of ICOS expression (right) gated on CD44^{hi} or CD44^{lo} CD4^{+} T cells at indicated tissues from 9- to 10-week-old GF and AF mice (n = 3). (**B**) MFI of CD40 expression gated on DCs (Lin^{−} CD11c^{+} MHCII^{+}) or B cells at indicated tissues from 9- to 10-week-old GF and AF mice (n = 4 to 5). (**C** and **D**) GF mice (4.5 weeks old) were treated with isotype or anti-CD40L antibody every 3 days for 2.5 weeks (n = 3). (C) Representative histograms (left) and MFI of ICOS expression (right) gated on CD44^{hi} or CD44^{lo} CD4^{+} T cells at indicated tissues. (D) Representative FACS plot of CXCR5 and PD-1 (left) and frequency of PD-1^{hi} CXCR5^{+} T_{FH} cells (right) gated on CD4^{+} TCRβ^{+} Foxp3^{−} CD44^{hi} cells. (**E**) Number of T_{FH} cells in indicated tissues from GF mice treated with isotype and anti-CD40L antibody. (**F**) Total serum IgE levels in GF mice treated with isotype and anti-CD40L antibody. Each symbol represents an individual mouse. Data in (A) and (C) to (F) are representative of three independent experiments. Data were pooled from two independent experiments (B). Statistical differences were determined by two-way ANOVA with Tukey's multiple comparisons test. *$P < 0.05$, **$P < 0.01$, ***$P < 0.001$. Error bars represent SEM.

In contrast, B cell–derived signals are not required for ICOS up-regulation in CD4+ T cells. Although B cells constitutively express CD40 (20), ICOS expression levels on activated CD4+ T cells from MLN and PP of GF B cell–deficient $Jh^{-/-}$ mice were comparable to those in GF wild-type (WT) mice (fig. S4B). These results collectively indicate that CD40 expressed on DCs, but not on B cells, in MLN and PP plays a critical role in ICOS up-regulation on food Ag–reactive T cells and consequent differentiation of T_FH cells in GF conditions.

B cells are also indispensable for the generation of food Ag–driven T_FH cells in GF mice

Previous studies showed that B cells are involved in the generation of T_FH cells. Thus, the lack of Ag presentation by B cells to cognate T cells causes defective T_FH cell generation (21). In addition, ICOSL expressed on B cells is required for T_FH cell generation (22). Despite the dispensable role of B cells in ICOS up-regulation on activated CD4+ T cells, the generation of food Ag–driven T_FH cells in GF mice was profoundly defective in GF $Jh^{-/-}$ mice (fig. S6, A and B).

To further address the relative contribution of Ag presentation and ICOSL provided by B cells to the development of food Ag–driven T_FH cells in GF mice, we generated mixed bone marrow chimeras (BMCs) to make major histocompatibility complex (MHC) II and ICOSL expression defective only on B cells, but not on the other Ag-presenting cells such as CD11c+ DCs (fig. S7A). T_FH cell populations in MLN and PP were deficient in mixed BMCs with B cell–specific ablation of both MHCII and ICOSL (fig. S7, B and C). Consequently, GC B cell generation and IgE elevation were defective in both mixed BMCs (fig. S7, D and E). However, whereas CXCR5+ cell generation was defective in ICOSL$^{-/-}$ BMC, CXCR5+ population was significantly higher in MHCII$^{-/-}$ BMC than in ICOSL$^{-/-}$ BMC (fig. S7F). These results indicate that B cell–derived ICOSL signaling is required for the generation of CXCR5+ T cells at an early stage of food Ag–driven T_FH cell differentiation and the presentation of cognate Ags by B cells is required for further differentiation of CXCR5+ T cells into GC T_FH cells. Together, our results indicate that DCs and B cells exert different roles in stepwise differentiation of food Ag–driven T_FH cells in GF mice.

Food Ag–induced T_FH cells are generated more efficiently at early age than at adult age

As shown previously, the generation of food Ag–driven T_FH cells in GALT was effectively prevented by the treatment with anti-ICOSL antibody. After the cessation of anti-ICOSL antibody treatment, we kept tracking T_FH cell populations (Fig. 4A). We found that the recovery of T_FH cells was profoundly retarded and T_FH cells were not fully re-covered even at 4 weeks after cessation of anti-ICOSL treatment (Fig. 4, B and C). Consistent with the levels of T_FH cells, serum IgE levels were not effectively increased relative to age-matched control (Fig. 4D). Because T_FH cell differentiation occurred rapidly in MLN and PP of young GF mice weaned onto NCD (fig. S2A), these results suggest that food Ag–induced T_FH cell generation is not efficient in adult mice relative to young mice, i.e., GF mice at weaning period.

To further support these findings, we compared young AF mice with adult AF mice, both switched to NCD. T_FH cells were efficiently generated in GALT of young AF mice fed with NCD (Fig. 4, E and F). Upon the exposure to NCD for the same period of 4 weeks, CD44^{hi} activated CD4+ T cells were comparable between young and adult AF mice (fig. S8, A and B). Although adult AF mice switched to NCD showed increased levels of GATA3-expressing T_H2 cells in MLN and PP (fig. S8C), T_FH cell generation was profoundly limited

in adult AF mice exposed to NCD (Fig. 4, E and F). Paralleling T_FH cell frequency in MLN and PP, serum IgE levels were lower in adult AF mice than in young AF mice exposed to NCD (Fig. 4G). These results support the idea that the host immune response to ingested food Ags in GF mice at an early age is highly favorable to T_FH cell generation relative to adult mice and IL-4–producing T_FH cells, rather than T_H2 cells, are more important in spontaneous IgE elevation driven by food Ags. Furthermore, these results also suggest that the abundant T_FH cells in MLN and PP of adult GF mice are maintained by prolonged survival of T_FH cells generated in early life rather than replenishment by newly generated T_FH cells.

Food Ag–driven T_FH cells require cognate Ags and ICOS signaling for their maintenance

To test whether continuous exposure to food Ags is required for maintaining T_FH cells, we fed adult GF mice with AFD to remove contact with food Ags, because de novo food Ag–driven T_FH cell generation is not efficient at the adult stage. As a consequence, T_FH cell populations shrank to about 40% relative to those in GF mice (Fig. 5A), indicating partial dependence on contact with cognate Ags. A considerable proportion of T_FH cells survived even after depriving exposure to food Ags, presumably representing the presence of long-lived memory T_FH cells (Fig. 5A). These results demonstrate that food Ag–induced T_FH cells are heterogeneous with regard to the requirement of contact with Ags for their maintenance.

Maintenance of T_FH cells generated after Ag immunization is known to depend on ICOS-ICOSL interaction (18). To examine this requirement for food Ag–driven T_FH cells, we treated adult GF mice with anti-ICOSL antibody at 12 weeks of age. After preventing ICOS-ICOSL interaction, T_FH cell frequencies quickly declined to the basal level seen in AF mice (Fig. 5B), indicating that ICOS-ICOSL interaction is essential for the maintenance of food Ag–induced T_FH cells in GF mice.

To examine whether B cells are also required for the maintenance of food Ag–driven T_FH cells, we depleted B cells gradually in adult GF mice by injecting different doses of anti-CD20 antibody. At 2 weeks after B cell depletion, the frequency of T_FH cells correlated closely with the percentage of B cells in GALT, indicating that B cells are required for the maintenance of T_FH cells (Fig. 5C). Hence, we concluded that T cell receptor (TCR) stimulation by cognate Ags and ICOSL expressed on B cells collectively provide important survival signals to maintain T_FH cells residing in B cell follicles.

Long-lived IgE-producing plasma cells support prolonged high levels of serum IgE in GF mice

While T_FH cells were reduced in adult GF mice fed with AFD (Fig. 5A), serum IgE levels remained at a high level, although constant IgE elevation ceased with AFD feeding (Fig. 5D). Depletion of T_FH cells in adult GF mice by disrupting ICOS-ICOSL interaction for 3 weeks prevents IgE elevation (Fig. 5E), but IgE levels sustained higher than typical IgE levels in AF mice (Fig. 1A). Furthermore, serum IgE levels were not significantly reduced upon B cell depletion (Fig. 5F). As the half-life of mouse IgE is shorter than 48 hours (1), our observations suggest that long-lived IgE-producing plasma cells are responsible for sustaining high levels of serum IgE in T_FH cell–depleted GF mice without the need for de novo generation of IgE-producing cells. Long-lived plasma cells are known to be radioresistant (23). In this respect, serum IgE levels could persist for 2 weeks even in adult GF mice lethally irradiated and reconstituted with BM cells from $Rag1^{-/-}$ mice (fig. S9, A and B). Also, irradiation-resistant
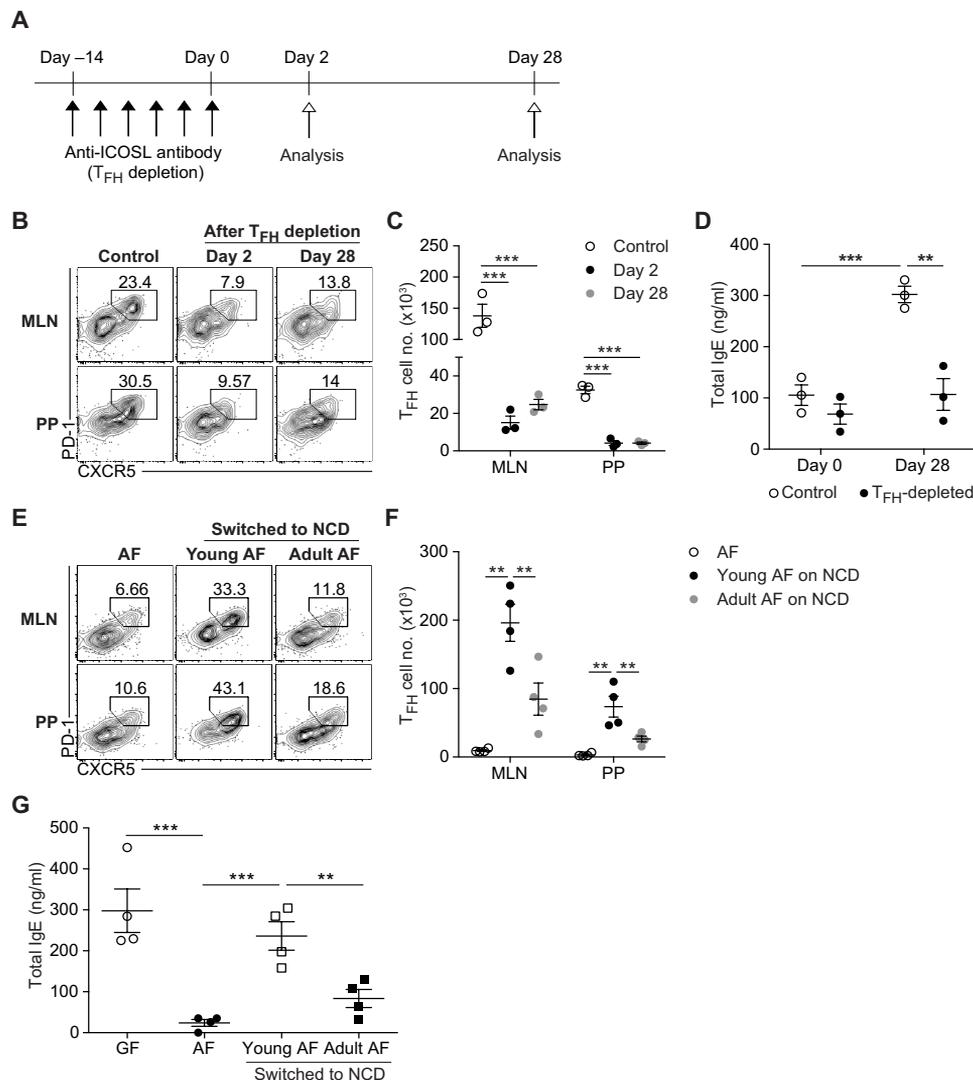
Fig. 4. T_{FH} cell generation and IgE elevation in response to food Ags are developmentally regulated. (A to **D**) GF mice (6.5 weeks old) were treated with anti-ICOSL antibody for 2 weeks to deplete T_{FH} cells. Mice were analyzed to examine the level of T_{FH} cells at days 2 and 28 after cessation of anti-ICOSL antibody treatment ($n = 3$). (A) Schematic view of experimental design and time plan. (B) Representative FACS plots of PD-1 and CXCR5 gated on CD4$^+$ TCRβ$^+$ Foxp3$^-$ CD44^{hi} cells. (C) Number of PD-1^{hi} CXCR5$^+$ T_{FH} cells. (D) Serum IgE levels of control mice and mice with T_{FH} depletion at days 0 and 28 were measured by ELISA. (**E** to **G**) Young and adult AF mice (4 and 8 weeks of age, respectively) were switched to NCD for 4 weeks ($n = 4$). Representative FACS plots showing PD-1^{hi} CXCR5$^+$ T_{FH} cells gated on CD4$^+$ TCRβ$^+$ Foxp3$^-$ CD44^{hi} cells (E) and number of PD-1^{hi} CXCR5$^+$ T_{FH} cells (F) from MLN and PP of indicated mice. (G) Serum IgE levels in indicated mice by ELISA. Each symbol represents an individual mouse. All data are representative of two independent experiments. Statistical differences were determined by one-way (C, F, and G) or two-way (D) ANOVA with Tukey's multiple comparisons test. **$P < 0.01$, ***$P < 0.001$. Error bars represent SEM.

IgE-producing cells could survive in MLN and BM of lethally irradiated GF mice (fig. S9, C and D). Together, our results suggest that T_{FH} cells are essential for IgE elevation with age in GF mice but are not necessary for the maintenance of high level of serum IgE due to the generation of long-lived IgE-producing plasma cells.

Commensal microbiota restrains IgE elevation by suppressing aberrant host immune responses to food Ags
Next, to test the suppressive role of commensal microbes in T_{FH} cell generation and IgE production in response to food Ags, GF mice were colonized with commensal microbes by cohousing them with SPF mice. In these conventionalized GF (ConvGF) mice, colonization of commensal microbiota impaired food Ag–driven IgE elevation relative to age-matched GF mice (Fig. 6A). Nevertheless, serum IgE remained at a high level in ConvGF mice, presumably reflecting the production by long-lived plasma cells. IL-4–producing CD4$^+$ T cells in MLN and PP were reduced in ConvGF mice relative to GF mice (Fig. 6B).

Moreover, colonization of commensal microbiota resulted in the reduction of the frequency of preexisting food Ag–driven T_{FH} cells in MLN and PP of GF mice (Fig. 6C) despite the varied effects on the number of T_{FH} cells in MLN and PP (Fig. 6D). Especially, the number of IL-4–producing T_{FH} cells in MLN was profoundly reduced upon the microbial colonization (Fig. 6E). ICOS expression on activated CD4$^+$ T cells and CD40 expression on DCs in GALT of SPF mice were both comparable with those in GF mice (fig. S10). These results suggest that commensal microbiota–mediated suppression of IgE
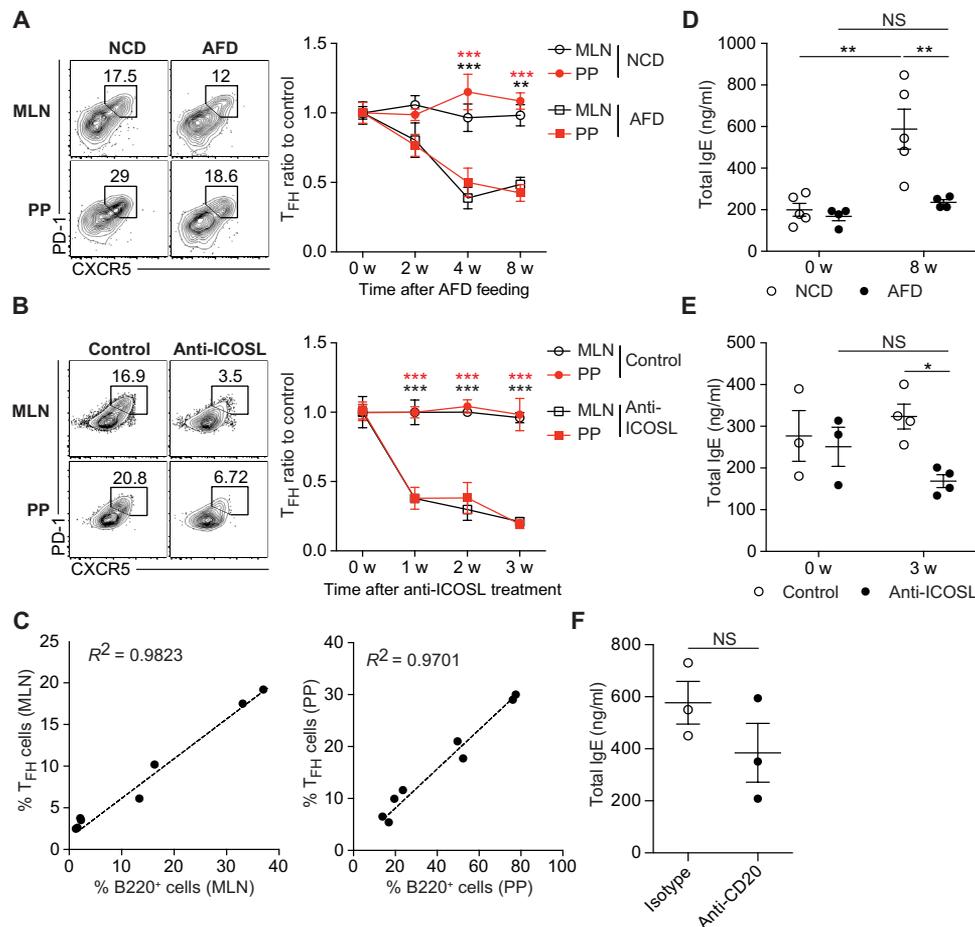
Fig. 5. Long-lived IgE-producing plasma cells contribute to sustained serum IgE levels regardless of the maintenance of T_{FH} cells in adult mice. (**A** and **D**) GF mice (10 to 12 weeks old) were fed with NCD and AFD for 8 weeks (NCD versus AFD, $n = 4$ to 5). (A) Representative FACS plots showing PD-1^{hi} CXCR5$^+$ T_{FH} cells gated on CD4$^+$ TCRβ$^+$ Foxp3$^-$ CD44^{hi} cells in MLN and PP (left) and ratios of T_{FH} cell frequency (right). (**B** and **E**) GF mice (12 weeks old) were untreated or treated with anti-ICOSL antibody every 3 days for 3 weeks (control versus anti-ICOSL, $n = 4$). (B) Representative FACS plots showing T_{FH} cells in MLN and PP (left) and ratios of T_{FH} cell frequency (right). (**C**) B cells in 10-week-old GF mice were gradually depleted by treating once with 0, 25, 100, and 250 μg of anti-CD20–depleting antibody ($n = 2$ per each dose). The correlation between the frequency of T_{FH} cells and B220$^+$ cells in MLN (left) and PP (right) was examined at 2 weeks after anti-CD20 antibody treatment. (D) Serum IgE levels in GF control (NCD, $n = 5$) and GF on AFD (AFD, $n = 4$) for indicated periods. (E) Serum IgE levels in GF untreated control ($n = 3$) and GF mice treated with anti-ICOSL antibody for indicated periods ($n = 4$). (**F**) GF mice (14 weeks old) were treated with isotype and anti-CD20 antibody (250 μg) every 3 days for 2 weeks. Serum IgE levels were shown. Each symbol represents an individual mouse. Data in (A) to (D) are pooled from two or three independent experiments. Data in (E) and (F) are representative of two independent experiments. Statistical differences were determined by two-way (A, B, D, and E) ANOVA with Tukey's multiple comparisons test and by unpaired two-tailed Student's t test (F). *$P < 0.05$, **$P < 0.01$, ***$P < 0.001$. NS, not significant. Error bars represent SEM.

elevation and T_{FH} cell generation is not mediated by altered expression of costimulatory molecules on both CD4$^+$ T cells and DCs. Collectively, our data indicate that the reduction of IL-4–producing T_{FH} cells is responsible for the cessation of IgE elevation in ConvGF mice.

To examine whether IgE elevation by ABX-mediated disruption of commensal microbiota is also dependent on food Ags, young SPF mice were weaned onto AAD and simultaneously treated with ABX. In accordance with a previous report (*2*), ABX treatment led to the elevation of serum IgE (Fig. 6F). As observed in GF mice, ABX treatment led to the increase of T_{FH} cells more prominently in MLN (Fig. 6G). Furthermore, deprivation of food Ags during ABX treatment resulted in the reduction of both serum IgE levels and T_{FH} cells in MLN and PP (Fig. 6, F and G). Collectively, these results demonstrate that IgE elevation occurring by disruption of commensal microbiota is mediated by an aberrant host immune response to ingested food Ags.

DISCUSSION
In this study, we have demonstrated that spontaneous IgE elevation in GF and ABX-treated mice is driven by T_{FH} cells generated in response to exogenous food Ags in MLN and PP of GF mice and that food Ag–driven T_{FH} cells are a major source of IL-4, a cytokine essential for IgE class switching (*15*). In a previous study, spontaneous IgE elevation in GF mice was maintained when these mice were fed with hydrolyzed infant formula as a source of AFD (*5*). However, in our hands, we were unable to stably raise GF mice on the same infant formula. Because of the lack of sufficient information about the exact composition of this formula, we are unable to offer a definitive explanation for this discrepancy. However, it is plausible that the proteins in the infant formula are only partially hydrolyzed. In this regard, the amount of non-hydrolyzed protein in the infant formula might be sufficient to induce IgE elevation in GF mice despite a
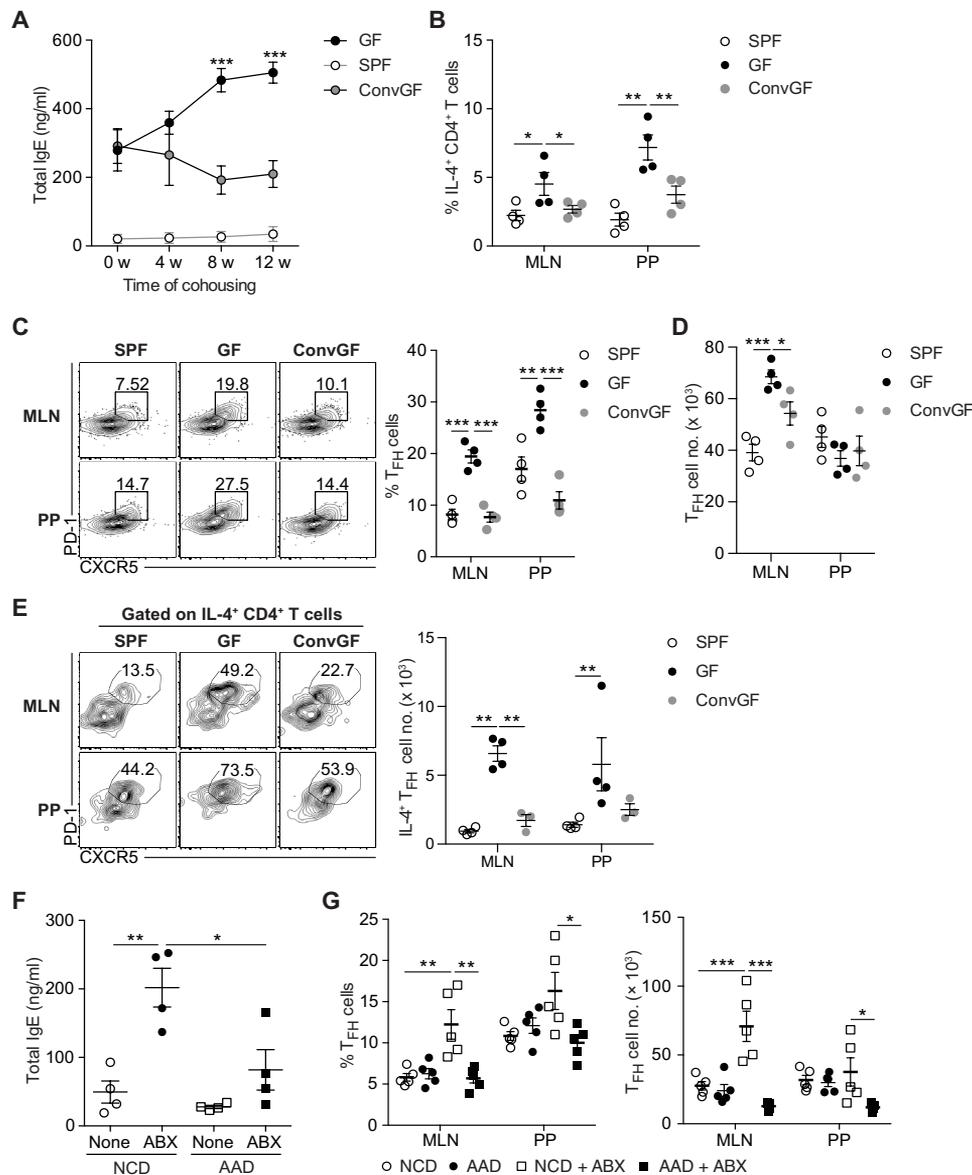
Fig. 6. Commensal microbiota suppresses IgE elevation by restraining food Ag–driven T_{FH} cell generation. (**A** to **C**) GF mice (10 weeks old) were conventionalized by cohousing them with SPF mice for indicated periods (ConvGF). (A) Serum IgE levels in age-matched SPF, GF, and ConvGF mice at the indicated time point after conventionalization were measured by ELISA ($n = 3$). (B) Frequency of IL-4^{+} cells among CD44^{hi} CD4^{+} T cells in MLN and PP from indicated mice at 8 weeks after conventionalization ($n = 4$). (C) Representative FACS plots of PD-1 and CXCR5 (left) and frequency of PD-1^{hi} CXCR5^{+} T_{FH} cells gated on CD4^{+} TCRβ^{+} Foxp3^{−} CD44^{hi} cells in MLN and PP from indicated mice (right) ($n = 4$). (**D**) Number of T_{FH} cells in MLN and PP from indicated mice. (**E**) Representative FACS plots showing the frequency of PD-1^{hi} CXCR5^{+} T_{FH} cells gated on IL-4–producing CD4^{+} T cells (left) and number of IL-4–producing T_{FH} cells (right). (**F** and **G**) SPF mice were weaned onto either NCD or AAD and were untreated or simultaneously treated with broad-spectrum ABX in drinking water for 6 weeks. (F) Serum IgE levels by ELISA ($n = 4$). (G) Frequency of PD-1^{hi} CXCR5^{+} T_{FH} cells gated on CD4^{+} TCRβ^{+} Foxp3^{−} CD44^{hi} cells (left) and number of T_{FH} cells (right) in MLN and PP from indicated mice ($n = 5$). Each symbol represents an individual mouse. All data in (A) to (F) are representatives of two independent experiments, and data in (G) are pooled from two independent experiments. Statistical differences were determined by one-way (A to E and G) or two-way (F) ANOVA with Tukey's multiple comparisons test. *$P < 0.05$, **$P < 0.01$, ***$P < 0.001$. Error bars represent SEM.

trend toward reduced levels of IgE in GF mice fed with infant formula (5). Nevertheless, our findings collectively indicate that food Ags are critical for the spontaneous IgE elevation in GF and ABX-treated mice. First, GF and ABX-treated mice devoid of contact with food Ags by raising mice on laboratory-made AFD or commercially available AAD consistently displayed low levels of serum IgE. Second, IgE elevation in GF and ABX-treated mice was mediated by T_{FH} cells in GALT, their generation being profoundly impaired in mice raised on

AFD. Third, our data from GF mice raised on several diets showed different effects of individual food Ag on the generation of T_{FH} cells in GALT and IgE elevation. These data provide compelling evidence for the causative role of food Ags in spontaneous IgE elevation in GF conditions.

Why do ingested food Ags lead to the generation of $T_{H}2$-skewed T_{FH} cells and subsequent IgE elevation in mice with disrupted commensal microbiota? We believe that multiple mechanisms are involved. Some food Ags might be resistant to the digestive enzymes

derived from the host, thereby leading to effective recognition by the host immune systems (*24*). In this respect, wheat gluten, which was shown to be digestion resistant (*25*), induced IgE elevation effectively under GF conditions. In addition, food Ags in NCD might have intrinsic immunogenic properties as shown in DerP1 of house dust mites capable of inducing allergic responses (*26*). Such immunogenic food Ags might condition the intestinal environment to be more favorable for T_{FH} cell responses. In this respect, exposure to NCD, but not to AFD, might lead to the up-regulation of CD40 expressed on DCs in MLN and PP of GF mice. These mechanisms above are counterbalanced by the presence of commensal microbiota. In our results, GF mice showed elevated T_H2 responses in GALT relative to SPF mice. It was previously reported that commensal microbiota–derived RORγt$^+$ T_{reg} cells suppress aberrant T_H2 immune responses in the intestine (*27*). Hence, immune responses to ingested food Ags in GF and ABX-treated mice might be skewed to T_H2 responses due to impaired RORγt$^+$ T_{reg} cell generation. Moreover, as seen in SPF mice, the presence of commensal microbiota suppresses the generation of T_{FH} cells and prevents IgE elevation in response to food Ags. Our results also revealed that colonization of GF mice with commensal microbiota rapidly deplete T_{FH} cells in GALT, resulting in cessation of IgE elevation. Collectively, the capacity of food Ags to induce IgE production is dependent on both intrinsic immunogenicity of food Ags and the presence of commensal microbiota.

Food Ag–driven T_{FH} cell generation in GF mice occurs by a stepwise differentiation process. Initially, DCs in GALT of GF mice led to the up-regulation of ICOS expression on activated CD4$^+$ T cells through CD40-CD40L interaction and thereby promoted T_{FH} cell differentiation. Although the mechanism of selective regulation of CD40 by the exposure to NCD is largely unclear, the blockade of CD40-CD40L interaction led to the defective generation of T_{FH} cells in response to food Ags. Our data also established that B cells play an important role in the generation of food Ag–induced T_{FH} cells by providing ICOSL plus cognate Ags to the responding CD4$^+$ T cells. However, it was previously shown that the cotransfer of MHCII-deficient B cells and WT non-T_{reg} naïve CD4$^+$ T cells led to the increase of serum IgE in GF *Rag1*$^{-/-}$ mice (*5*). T_{FH} cell–independent mechanisms for IgE induction might be involved in this experimental setting. Donor CD4$^+$ T cells can activate and undergo homeostatic proliferation in GF *Rag1*$^{-/-}$ mice but at a slower tempo than those in SPF mice (*28*). Given that activated CD4$^+$ T cells are a major source of IL-2 (*29*) and IL-2 inhibits T_{FH} cell differentiation (*30*), this experimental setting might be more biased to represent T_{FH} cell–independent IgE induction. Therefore, we believed that BMC is more suitable to address the role of cognate Ag presentation by B cells in spontaneous IgE elevation.

The limited T_{FH} cell generation in adult AF mice exposed to food Ags and the slow tempo of T_{FH} cell recovery after T_{FH} cell depletion in adult GF mice indicate that food Ag–driven T_{FH} cell generation is less effective in adult than during young life. These data may explain why perturbation of microbiota at an early age is one of the critical factors influencing allergic diseases in human and, in particular, account for why the incidence of food allergy is higher in childhood than in adults (*4*). Further studies will be needed to resolve the issue why early life is highly vulnerable to food Ag–induced IgE elevation by perturbing microbiota.

In keeping with the limited de novo food Ag–driven T_{FH} cell generation in adults, most T_{FH} cells residing in GALT of adult GF mice were the progeny of T_{FH} cells made during the weaning stage. Profound depletion of those T_{FH} cells by treatment with B cell–

depleting antibody indicated that B cells provide a major survival signal for the maintenance of food Ag–driven T_{FH} cells in GF mice. Blocking ICOS-ICOSL interaction was more efficient at depleting T_{FH} cells in adult GF mice than deprivation of contact with food Ags. Because Ag-bearing B cells express ICOSL, we envisage that ICOS-ICOSL interaction between T_{FH} cells and B cells in B cell follicles is a crucial survival signal for maintaining food Ag–driven T_{FH} cells. Furthermore, the finding that a considerable fraction of T_{FH} cells survived without contact with food Ags presumably signifies the generation of long-lived T_{FH} memory cells, in addition to Ag-dependent short-lived T_{FH} cells.

It is notable that high serum IgE levels in GF mice were sustained despite T_{FH} cell depletion, colonization with commensal microbiota, and heavy irradiation. These data indicated that long-lived IgE-producing plasma cells are a major contributor to sustained levels of serum IgE in GF mice. Although long-lived plasma cells are generally found in BM (*23*), we found IgE-producing long-lived plasma cells in both MLN and BM of GF mice. Hence, MLN is a major site for IgE elevation through both de novo synthesis by B cells and residence of long-lived IgE-producing plasma cells. On this point, long-lived IgE-producing plasma cells are generated by the GC reaction, whereas extrafollicular IgE production is mediated by short-lived plasma cells (*1*). Therefore, our data on the presence of long-lived plasma cells further support the critical role of T_{FH} cell–mediated GC reactions in spontaneous IgE elevation in GF mice. Furthermore, the presence of long-lived plasma cells also explains why serum IgE levels were still high despite a decrease in T_{FH} cells induced by colonization of commensal microbes in adult mice.

GF mice are more susceptible to food allergy as well as allergic airway inflammation relative to SPF mice upon allergen sensitization (*2*, *31*). A clinical report showed that high levels of serum IgE correlate closely with the prevalence of allergic disease (*32*). Further extending these findings, IgE spontaneously elevated in response to food Ags might be a key contributing factor for increasing the susceptibility to allergic responses in the absence of commensal microbiota. Hence, our demonstration of aberrant IgE elevation in GF and ABX-treated mice reflecting enhanced generation of T_H2-skewed T_{FH} cells against food Ags explains why disruption of commensal microbiota is causally linked with the high risk of allergic diseases.

MATERIALS AND METHODS
Mice
SPF C57BL/6, *Rag1*$^{-/-}$, *Icosl*$^{-/-}$ and *H2-Ab1*$^{-/-}$ (MHCII-deficient) mice were purchased from The Jackson Laboratory and maintained in the animal facility of POSTECH Biotech Center in accordance with institutional ethical guideline. GF C57BL/6, *Jh*$^{-/-}$, and *Rag1*$^{-/-}$ mice were provided by A. Macpherson and K. McCoy (University of Bern, Switzerland). GF mice were maintained in sterile flexible film isolators (Class Biological Clean Ltd.) by feeding autoclaved Teklad global 18% protein rodent diets (catalog no. 2018S, Envigo). AF mice were generated and maintained as previously described (*13*). All animal studies were performed in accordance with the guidelines of the Institutional Animal Care and Use Committee of POSTECH.

Antibiotics treatment
To disrupt commensal microbiota, SPF mice were fed with drinking water containing ampicillin (1 g/liter), neomycin (1 g/liter), metronidazole (1 g/liter), and vancomycin (0.5 g/liter) ad libitum.

Cell isolation

Lymph nodes, spleen, and PPs were collected, and single-cell suspensions were generated by mechanical disruption. For isolating DCs, collected tissues were minced with razor blade and further digested with deoxyribonuclease I and collagenase D for 45 min at 37°C in RPMI 1640 containing fetal bovine serum (FBS) (3%, v/v), HEPES buffer (20 mM), penicillin (100 U/ml), streptomycin (100 µg/ml), sodium pyruvate (1 mM), and nonessential amino acids (1 mM). Small intestinal lamina propria cells were isolated as previously described (*13*).

Flow cytometry

Fluorescent dye–labeled antibodies for BCL-6 (K112-91), B220 (RA3-6B2), CD4 (RM4-5), CD11b (M1/70), CD11c (N418), CD40 (3/23), CD44 (IM7), CD80 (16-10A1), CD86 (GL1), CD90.1 (OX-7), CD103(2E7), CXCR5 (2G8), Foxp3 (FJK-16s), GATA3 (TWAJ), GL-7 (GL7), ICOS (C398.4A), ICOSL (HK5.3), IFN-γ (XMG1.2), IgD (11-26c.2a), IgE (RME-1), IL-4 (11B11), MHCII (M5/114.15.2), PD-1 (RMP1-30), and TCRβ (H57-597) were purchased from BD Biosciences, BioLegend, Thermo Fisher Scientific, and Tonbo Biosciences. For intracellular staining, surface-stained cells were fixed and permeabilized with Foxp3/ transcription factor staining buffer set (Thermo Fisher Scientific). For intracellular cytokine staining, cells were stimulated with cell stimulation cocktail plus protein transport inhibitors (Thermo Fisher Scientific) for 4 hours in RPMI 1640 containing 10% FBS, penicillin (100 U/ml), streptomycin (100 µg/ml), and 55 µM β-mercaptoethanol. Dead cells were excluded by Ghost Dye Violet 510 (Tonbo Biosciences). Stained cells were analyzed using LSRFortessa or FACSCanto II (BD Biosciences), and data were analyzed using FlowJo software (Tree Star).

In vivo depletion of T$_{FH}$ cells

GF mice were retro-orbitally injected with 150 µg (per mouse) of anti-ICOSL antibody (clone HK5.3, BioXCell) or anti-CD40L antibody (clone MR1, BioXCell) every 3 days for 2 to 3 weeks.

Adoptive cell transfer

For adoptive transfer of T$_{FH}$ cells and naïve B cells, live PD-1^{hi} CD4$^+$ CD25$^-$ CD44^{hi} population and B220$^+$ GL-7$^-$ cells from MLNs and spleen were fluorescence-activated cell sorting (FACS)–sorted with MoFlo Astrios (Beckman Coulter). Sorted T$_{FH}$ cells (0.2×10^6) and sorted B cells (5×10^6) were simultaneously transferred into *Rag1*$^{-/-}$ mice by retro-orbital injection.

Bone marrow chimeras

For generating mixed BMCs, 8- to 10-week-old GF *Jh*$^{-/-}$ mice were transferred to an autoclaved plastic cylinder sealed with Mylar film. The cylinder-containing GF mice were irradiated with a lethal dose of 900 cGy using X-RAD 320 (Precision X-ray). Irradiated recipient mice were transferred to the isolator and reconstituted with 5×10^6 mixed BM cells. BM cells from *Jh*$^{-/-}$ mice were mixed with BM cells from either *Icosl*$^{-/-}$ or *H2-Ab1*$^{-/-}$ mice in an 8:2 ratio. An 8:2 mixture of *Jh*$^{-/-}$ BM cells and WT B6 BM cells was transferred into irradiated GF *Jh*$^{-/-}$ mice as a control. At 6 weeks after reconstitution, BMCs were analyzed. For elucidating the role of long-lived IgE-producing cells in sustained IgE responses, 14-week-old GF B6 mice were similarly irradiated with 900 cGy and reconstituted with BM cells from *Rag1*$^{-/-}$ mice to deplete lymphocytes.

Preparation of custom diets

For wheat gluten and peanut diet, wheat gluten (Sigma-Aldrich) and ground peanut were mixed with amino-acid diet (catalog no. TD99366, Envigo) and autoclaved for feeding AF mice in GF condition. Gluten and ground peanut were adjusted to occupy 20 to 30% of total weights. For casein and EW diet, we purchased sterile and vacuum-packed purified protein diet containing 20% of each protein based on protein-free diet from Envigo. Three-week-old AF pups were weaned onto these custom diets for 6 to 8 weeks.

ELISA for IgE measurement

For measuring total IgE in serum, an enzyme-linked immunosorbent assay (ELISA) plate was coated with purified monoclonal anti-mouse IgE antibody (RME-1, BioLegend) for 2 hours at room temperature (RT). Then, the plate was incubated with blocking buffer [5% FBS in phosphate-buffered saline (PBS)] for 1 hour. After blocking, the plate was washed, and diluted sera and standards were incubated for 2 hours at RT. Horseradish peroxidase–conjugated polyclonal anti-mouse IgE (Southern Biotech) was used as a detection antibody. After a 2-hour incubation with a detection antibody, peroxidase reaction was visualized by adding tetramethylbenzidine (TMB) substrate solution (SurModics). Plates were read at 405 nm using a spectrophotometer. For measuring food Ag–specific IgE, NCD was grounded and incubated overnight in PBS to solubilize. Insoluble fraction was removed by filtering and centrifugation. Soluble fraction was collected and used as the diet extract. Protein concentration of soluble fraction was measured by bicinchoninic acid (BCA) assay (Thermo Fisher Scientific). Diet extract (0.5 mg/ml) and control protein (OVA) were coated on an ELISA plate. To enhance the detection of Ag-specific IgE in sera, IgG in sera was depleted by coincubation of protein A/G (GE Healthcare). One-fifth diluted sera were incubated overnight at 4°C, and ELISA was performed as described above.

ELISPOT for IgE-producing cells

Peripheral (inguinal, axillary, and cervical) lymph nodes, spleen, MLNs, and PPs in GF or AF mice were collected, and single-cell suspension was prepared. To enrich plasmablasts, lymphocytes were depleted by using biotinylated anti-B220 and anti-CD90.2 antibody and streptavidin-conjugated magnetic beads (BD Biosciences). Enriched cells (0.1×10^6 to 0.5×10^6) were added on an ELISPOT plate previously coated with anti-mouse IgE (RME-1, BioLegend). After 8 hours of incubation at 37°C, the plate was washed with PBS containing 2% Tween 20 and incubated with biotinylated monoclonal anti-mouse IgE (JKS-6, BioLegend) followed by streptavidin-conjugated alkaline phosphatase (BD Biosciences). Spots for IgE-producing cells were detected by addition of the bromochloroindolyl phosphate–nitro blue tetrazolium (BCIP-NBT) substrate (Sigma-Aldrich) solution.

Statistical analysis

All data were presented as means ± SEM. Data were analyzed by unpaired two-tailed Student's *t* test and one- or two-way ANOVA with Tukey's multiple comparisons test. Statistical analysis was performed using Prism 5 (GraphPad). *$P < 0.05$; **$P < 0.01$; ***$P < 0.001$.

SUPPLEMENTARY MATERIALS

Supplementary material for this article is available at http://advances.sciencemag.org/cgi/content/full/5/5/eaaw1507/DC1

Fig. S1. MLN and PP of GF mice are major sites for T$_H$2-skewed immune response against food Ags.
Fig. S2. T$_{FH}$ cells in MLN and PP of GF mice are generated upon weaning onto NCD, and AF mice displayed impaired generation of GC B cells and IgE-producing cells.
Fig. S3. Levels of wheat gluten–specific IgE in GF *Rag1*$^{-/-}$ mice cotransferred with naïve B cells and indicated CD4$^+$ T cell subsets.

Fig. S4. ICOS up-regulation on activated CD4$^+$ T cells is independent on the presence of T$_{FH}$ cells and B cells.

Fig. S5. Expression levels of CD80, CD86, and ICOSL on MLN and PP DCs are comparable between GF and AF mice.

Fig. S6. B cells are required for the generation of food Ag–driven T$_{FH}$ cells in GALT.

Fig. S7. B cells promote terminal differentiation of food Ag–driven T$_{FH}$ cells by providing ICOS signaling and presenting cognate Ags.

Fig. S8. Levels of CD4$^+$ T cell activation in MLN and PP are comparable between young and adult AF mice switched to NCD, but the latter shows increased levels of T$_H$2 cells.

Fig. S9. High serum IgE levels in adult GF mice are sustained by radioresistant long-lived IgE-producing cells in MLN and BM.

Fig. S10. ICOS expression on activated CD4$^+$ T cells and CD40 expression on DCs in MLN and PP in SPF mice are both comparable with those in GF mice.

REFERENCES AND NOTES

1. L. C. Wu, A. A. Zarrin, The production and regulation of IgE by the immune system. *Nat. Rev. Immunol.* **14**, 247–259 (2014).
2. D. A. Hill, M. C. Siracusa, M. C. Abt, B. S. Kim, D. Kobuley, M. Kubo, T. Kambayashi, D. F. LaRosa, E. D. Renner, J. S. Orange, F. D. Bushman, D. Artis, Commensal bacteria-derived signals regulate basophil hematopoiesis and allergic inflammation. *Nat. Med.* **18**, 538–546 (2012).
3. T. Kawakami, J. Kitaura, Mast cell survival and activation by IgE in the absence of antigen: A consideration of the biologic mechanisms and relevance. *J. Immunol.* **175**, 4167–4173 (2005).
4. S.-W. Hong, K. S. Kim, C. D. Surh, Beyond hygiene: Commensal microbiota and allergic diseases. *Immune Netw.* **17**, 48–59 (2017).
5. J. Cahenzli, Y. Köller, M. Wyss, M. B. Geuking, K. D. McCoy, Intestinal microbial diversity during early-life colonization shapes long-term IgE levels. *Cell Host Microbe* **14**, 559–570 (2013).
6. S. Crotty, T follicular helper cell differentiation, function, and roles in disease. *Immunity* **41**, 529–542 (2014).
7. R. Goenka, L. G. Barnett, J. S. Silver, P. J. O'Neill, C. A. Hunter, M. P. Cancro, T. M. Laufer, Cutting edge: Dendritic cell-restricted antigen presentation initiates the follicular helper T cell program but cannot complete ultimate effector differentiation. *J. Immunol.* **187**, 1091–1095 (2011).
8. Y. S. Choi, R. Kageyama, D. Eto, T. C. Escobar, R. J. Johnston, L. Monticelli, C. Lao, S. Crotty, ICOS receptor instructs T follicular helper cell versus effector cell differentiation via induction of the transcriptional repressor Bcl6. *Immunity* **34**, 932–946 (2011).
9. C. G. Vinuesa, J. G. Cyster, How T cells earn the follicular rite of passage. *Immunity* **35**, 671–680 (2011).
10. T. Kobayashi, K. Iijima, A. L. Dent, H. Kita, Follicular helper T cells mediate IgE antibody response to airborne allergens. *J. Allergy Clin. Immunol.* **139**, 300–313.e7 (2017).
11. A. P. Meli, G. Fontés, C. Leung Soo, I. L. King, T follicular helper cell-derived IL-4 is required for IgE production during intestinal helminth infection. *J. Immunol.* **199**, 244–252 (2017).
12. B. H. Ye, G. Cattoretti, Q. Shen, J. Zhang, N. Hawe, R. de Waard, C. Leung, M. Nouri-Shirazi, A. Orazi, R. S. K. Chaganti, P. Rothman, A. M. Stall, P.-P. Pandolfi, R. Dalla-Favera, The *BCL-6* proto-oncogene controls germinal-centre formation and Th2-type inflammation. *Nat. Genet.* **16**, 161–170 (1997).
13. K. S. Kim, S.-W. Hong, D. Han, J. Yi, J. Jung, B.-G. Yang, J. Y. Lee, M. Lee, C. D. Surh, Dietary antigens limit mucosal immunity by inducing regulatory T cells in the small intestine. *Science* **351**, 858–863 (2016).
14. K. D. McCoy, N. L. Harris, P. Diener, S. Hatak, B. Odermatt, L. Hangartner, B. M. Senn, B. J. Marsland, M. B. Geuking, H. Hengartner, A. J. S. Macpherson, R. M. Zinkernagel, Natural IgE production in the absence of MHC Class II cognate help. *Immunity* **24**, 329–339 (2006).
15. R. S. Geha, H. H. Jabara, S. R. Brodeur, The regulation of immunoglobulin E class-switch recombination. *Nat. Rev. Immunol.* **3**, 721–732 (2003).
16. A. Ballesteros-Tato, T. D. Randall, F. E. Lund, R. Spolski, W. J. Leonard, B. León, T follicular helper cell plasticity shapes pathogenic T helper 2 cell-mediated immunity to inhaled house dust mite. *Immunity* **44**, 259–273 (2016).
17. A. G. Zaretsky, J. J. Taylor, I. L. King, F. A. Marshall, M. Mohrs, E. J. Pearce, T follicular helper cells differentiate from Th2 cells in response to helminth antigens. *J. Exp. Med.* **206**, 991–999 (2009).
18. J. P. Weber, F. Fuhrmann, R. K. Feist, A. Lahmann, M. S. al Baz, L.-J. Gentz, D. Vu van, H. W. Mages, C. Haftmann, R. Riedel, J. R. Grün, W. Schuh, R. A. Kroczek, A. Radbruch, M.-F. Mashreghi, A. Hutloff, ICOS maintains the T follicular helper cell phenotype by down-regulating Krüppel-like factor 2. *J. Exp. Med.* **212**, 217–233 (2015).
19. H. Akiba, K. Takeda, Y. Kojima, Y. Usui, N. Harada, T. Yamazaki, J. Ma, K. Tezuka, H. Yagita, K. Okumura, The role of ICOS in the CXCR5$^+$ follicular B helper T cell maintenance in vivo. *J. Immunol.* **175**, 2340–2348 (2005).
20. S. A. Quezada, L. Z. Jarvinen, E. F. Lind, R. J. Noelle, CD40/CD154 interactions at the interface of tolerance and immunity. *Annu. Rev. Immunol.* **22**, 307–328 (2004).
21. M. W. Dahlgren, M. Gustafsson-Hedberg, M. Livingston, H. Cucak, S. Alsén, U. Yrlid, B. Johansson-Lindbom, T follicular helper, but not Th1, cell differentiation in the absence of conventional dendritic cells. *J. Immunol.* **194**, 5187–5199 (2015).
22. K. M. Hamel, Y. Cao, S. A. Olalekan, A. Finnegan, B cell-specific expression of inducible costimulator ligand is necessary for the induction of arthritis in mice. *Arthritis Rheum.* **66**, 60–67 (2014).
23. M. K. Slifka, R. Antia, J. K. Whitmire, R. Ahmed, Humoral immunity due to long-lived plasma cells. *Immunity* **8**, 363–372 (1998).
24. E. Untersmayr, E. Jensen-Jarolim, The role of protein digestibility and antacids on food allergy outcomes. *J. Allergy Clin. Immunol.* **121**, 1301–1308 (2008).
25. T. Rahaman, V. Vasiljevic, L. Ramchandran, Shear, heat and pH induced conformational changes of wheat gluten—Impact on antigenicity. *Food Chem.* **196**, 180–188 (2016).
26. C. Traidl-Hoffmann, T. Jakob, H. Behrendt, Determinants of allergenicity. *J. Allergy Clin. Immunol.* **123**, 558–566 (2009).
27. C. Ohnmacht, J.-H. Park, S. Cording, J. B. Wing, K. Atarashi, Y. Obata, V. Gaboriau-Routhiau, R. Marques, S. Dulauroy, M. Fedoseeva, M. Busslinger, N. Cerf-Bensussan, I. G. Boneca, D. Voehringer, K. Hase, K. Honda, S. Sakaguchi, G. Eberl, The microbiota regulates type 2 immunity through ROR rt+ T cells. *Science* **349**, 989–993 (2015).
28. W. C. Kieper, A. Troy, J. T. Burghardt, C. Ramsey, J. Y. Lee, H.-Q. Jiang, W. Dummer, H. Shen, J. J. Cebra, C. D. Surh, Recent immune status determines the source of antigens that drive homeostatic T cell expansion. *J. Immunol.* **174**, 3158–3163 (2005).
29. B. H. Nelson, IL-2, regulatory T cells, and tolerance. *J. Immunol.* **172**, 3983–3988 (2004).
30. A. Ballesteros-Tato, B. León, B. A. Graf, A. Moquin, P. S. Adams, F. E. Lund, T. D. Randall, Interleukin-2 inhibits germinal center formation by limiting T follicular helper cell differentiation. *Immunity* **36**, 847–856 (2012).
31. A. T. Stefka, T. Feehley, P. Tripathi, J. Qiu, K. McCoy, S. K. Mazmanian, M. Y. Tjota, G.-Y. Seo, S. Cao, B. R. Theriault, D. A. Antonopoulos, L. Zhou, E. B. Chang, Y.-X. Fu, C. R. Nagler, Commensal bacteria protect against food allergen sensitization. *Proc. Natl. Acad. Sci. U.S.A.* **111**, 13145–13150 (2014).
32. B. Burrows, F. D. Martinez, M. Halonen, R. A. Barbee, M. G. Cline, Association of asthma with serum IgE levels and skin-test reactivity to allergens. *N. Engl. J. Med.* **320**, 271–277 (1989).

Science Advances

Food antigens drive spontaneous IgE elevation in the absence of commensal microbiota

Sung-Wook Hong, Eunju O, Jun Young Lee, Minji Lee, Daehee Han, Hyun-Ja Ko, Jonathan Sprent, Charles D. Surh and Kwang Soon Kim

ARTICLE TOOLS	http://advances.sciencemag.org/content/5/5/eaaw1507
SUPPLEMENTARY MATERIALS	http://advances.sciencemag.org/content/suppl/2019/05/20/5.5.eaaw1507.DC1
REFERENCES	This article cites 32 articles, 12 of which you can access for free http://advances.sciencemag.org/content/5/5/eaaw1507#BIBL
PERMISSIONS	http://www.sciencemag.org/help/reprints-and-permissions

Use of this article is subject to the Terms of Service